

Photonics Breakthroughs 2024: Advances in Heavy-Metal-Free Quantum Dot Shortwave Infrared Photodetectors and Image Sensors: The Case of Ag₂Te QDs

Yongjie Wang  and Gerasimos Konstantatos 

Abstract—Shortwave infrared (SWIR) light holds promising applications spanning consumer electronics, industrial automation, and biomedical imaging. The detection of shortwave infrared light lays in the centre of SWIR applications. Conventional SWIR detectors rely on epitaxial semiconductors, which are costly and limited by low manufacturing throughput. Colloidal quantum dots (CQDs) have been developed to unravel these issues and comparable device performances have been achieved after decades' efforts. While CQDs can offer low-cost alternatives once high-volume maturity level is reached, their widespread adoption in consumer electronics market has been hindered also by concerns on the use of lead/mercury-based materials. Recent advances in heavy-metal-free CQDs, such as silver chalcogenides (Ag₂Te) and III-V semiconductors (InAs, InSb), have demonstrated performance metrics, which, in some cases, rival heavy-metal based counterparts. Progress in synthesis, surface passivation, and device engineering have enabled high detectivity ($>10^{12}$ Jones), broad spectral tunability (1000–2000 nm), monolithic integration with silicon readout circuits and proof of concept demonstration in image sensor and LIDAR use cases. These breakthroughs position heavy-metal-free CQDs as an environmentally compliant, scalable solution for next-generation SWIR technologies.

Index Terms—Colloidal quantum dots, heavy-metal-free, photodetectors, shortwave infrared.

I. INTRODUCTION

SHORTWAVE infrared (SWIR) light holds extraordinary potential for sensing and imaging, due to its penetrability in adverse atmospheric and weather conditions, and eye-safe characteristics [1], [2], [3]. SWIR photodetector makes

Received 22 April 2025; accepted 23 April 2025. Date of publication 28 April 2025; date of current version 27 May 2025. The work of Gerasimos Konstantatos was supported in part by the European Research Council (ERC) through the European Union's Horizon 2020 Research and Innovation Programme under Grant 101002306, in part by Fundació Privada Cellex through the Program CERCA and 'Severo Ochoa' Centre of Excellence under Grant CEX2019-000910-S, in part by Spanish State Research Agency, and in part by European Union under Grant 101119489 through 2DNeuralvision. (Corresponding author: Gerasimos Konstantatos.)

Yongjie Wang is with ICFO-Institut de Ciències Fotoniques, Castelldefels, 08860 Barcelona, Spain, and also with the Inorganic Chemistry Laboratory, University of Oxford, OX1 3QR Oxford, U.K. (e-mail: Yongjie.wang@alumni.icfo.eu).

Gerasimos Konstantatos is with ICFO-Institut de Ciències Fotoniques, Castelldefels, 08860 Barcelona, Spain, and also with ICREA-Institució Catalana de Recerca i Estudis Avançats, 08010 Barcelona, Spain (e-mail: gerasimos.konstantatos@icfo.eu.).

Digital Object Identifier 10.1109/JPHOT.2025.3564863

a cornerstone component in SWIR optoelectronics, enabling night vision, machine vision, defence and space applications, bio-imaging, industrial inspection techniques, 3D imaging and LIDAR applications [4], [5].

Current commercial SWIR photodetectors rely on epitaxial-grown materials, inevitably leading to high-cost and low manufacturing throughput. Furthermore, infrared imagers based on epitaxial materials face challenges towards small pixel, high-resolution sensor arrays due to complex integration processes involving flip-chip bonding. The high-cost and low manufacturing throughput has therefore contained infrared image sensors within military and industrial applications, leaving large-volume consumer-electronic market largely unexplored [6].

Semiconductor colloidal quantum dots (CQDs) have emerged as a cost-effective alternative material platform for high performance infrared photodetectors [7]. High responsivity and detectivity have been obtained with lead chalcogenide and mercury chalcogenide CQDs, as well as monolithic integration with Si CMOS ROICs for infrared image sensors, showing high throughput and high-resolution image sensors with largely reduced cost [8], [9], [10], [11], [12]. Yet, the toxicity of heavy metals, i.e., Pb and Hg, has raised concerns, barring the access of Pb or Hg based CQDs in consumer electronics products. Moreover, Restriction of Hazardous Substances (RoHS) regulations currently regulate the amount of heavy-metals (Cd, Pb, Hg) in consumer electronics. CQDs based on heavy-metal-free materials for non-toxic, low-cost, high-performance infrared photodetectors are thus urgently sought after [13], [14], [15]. This review highlights recent progress in heavy-metal-free CQDs, emphasizing their synthesis, device performance, and potential to democratize SWIR technologies. While several material compounds are briefly reviewed, the main focus of this work is on a recently emerged CQD material of Ag₂Te, that has demonstrated compelling performance and has been showcased for image sensor and LIDAR applications [16], [17].

II. BREAKTHROUGH RESEARCH

Recently, heavy-metal-free CQDs have shown rapid progress as promising candidates for high-performance, low-toxicity infrared photodetectors. Silver chalcogenide and III-V group CQDs have been synthesized with novel synthetic methods,

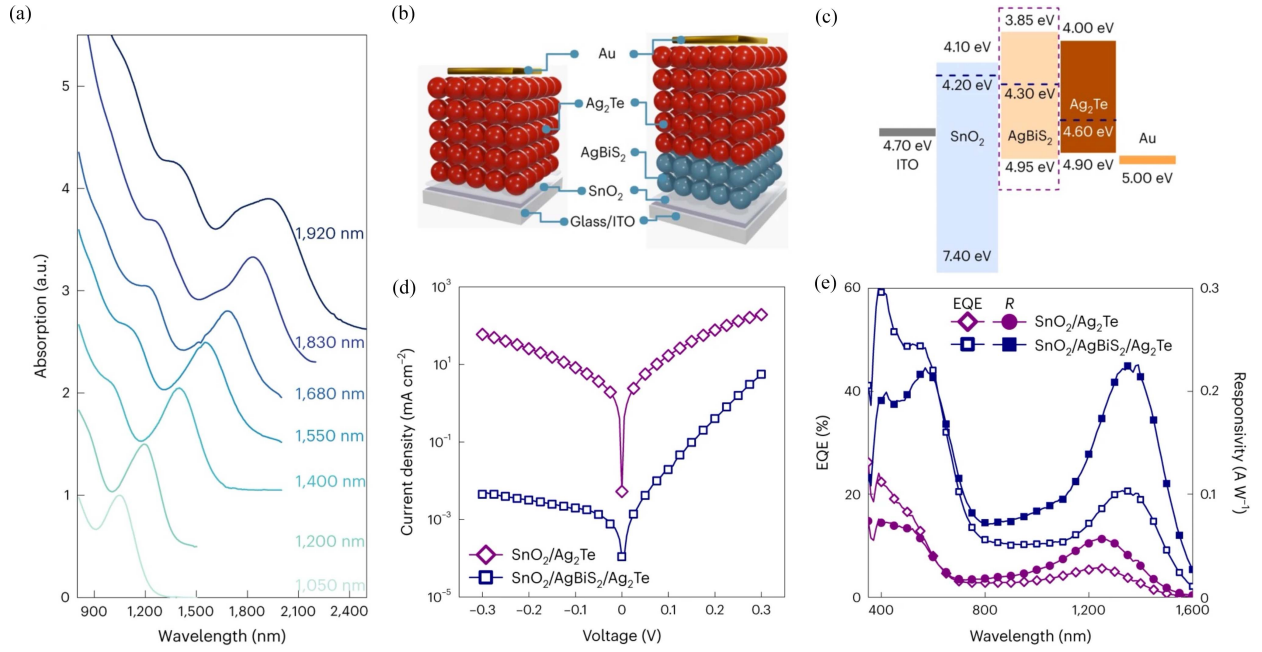


Fig. 1. (a) Absorption spectra of various-sized Ag_2Te QDs. (b) Schematic of the Ag_2Te QD photodiodes, with and without the AgBiS_2 NC buffer layer. (c) Dark current density–voltage (J – V) curves of photodiodes with and without a buffer layer. (d) EQE spectrum and responsivity (R) of Ag_2Te QD photodiodes with and without the AgBiS_2 NC buffer layer. Figures reproduced with permission from Springer Nature [16].

achieving monodispersed size dispersity and extraordinary size-tunability, resulting in a broad bandgap range covering from near infrared (NIR) to SWIR region [1], [18]. In the near infrared (NIR) region, AgBiS_2 and InAs CQDs have demonstrated extraordinary performances in both photovoltaic and detection devices, being the most promising solution-processable candidates for commercial NIR image sensors [19], [20], [21], [22], [23], [24]. SWIR Photodiodes based on heavy-metal-free CQDs have also been demonstrated with comparable performances with their heavy-metal counterparts, with specific detectivity over 10^{12} Jones reported [16]. Moreover, heavy-metal-free photodetectors have shown high-speed operation, with -3 dB bandwidth up to 6 MHz [25]. Monolithic integration with Si CMOS ROICs has been demonstrated successfully in lab-scale, showing heavy-metal-free and solution-processed SWIR imagers operating at room temperature [16], [26], [27]. These recent results have unleashed the potential of heavy-metal-free CQDs as novel RoHS-compliant infrared size-tunable optoelectronic materials, paving the way for the introduction of SWIR CQD technology into consumer electronics markets.

A. Ag_2Te CQDs for SWIR

Silver telluride (Ag_2Te) quantum dots have been studied for years targeting advanced bio-imaging applications, albeit achieving size tunability across the SWIR region has been challenging [1]. Large-sized Ag_2Te QDs with a photoluminescence peak exceeding 2000 nm were only obtainable using phosphine-induced ripening [34], [35], [36]. Yet the absence of distinct excitonic absorption peaks indicates insufficient control over energy landscapes in these CQDs, hindering the performance of optoelectronic devices [37], [38].

Recently, a phosphine-free synthesis method has been developed to overcome limitations in control of size uniformity and excitonic absorptions [16]. By eliminating phosphine-based ligands, the synthesis method enhances colloidal stability, reduces energetic disorder, and enables precise size tuning (800–2000 nm) with distinct excitonic peaks (Fig. 1(a)).

These high-quality Ag_2Te CQDs were further integrated with SnO_2 and AgBiS_2 nanocrystals (NCs) buffer layers (Fig. 1(b) and (c)), forming a heterojunction photodiode. Devices with AgBiS_2 NC buffer layer showed substantially reduced reverse bias dark current (Fig. 1(d)) and improved external quantum efficiency (EQE, Fig. 1(e)). The Ag_2Te CQD photodetectors exhibit exceptional performance metrics: a linear dynamic range (LDR) over 118 dB (Fig. 2(a)), a -3 dB bandwidth of 110 kHz (Fig. 2(b)) and a room-temperature specific detectivity (D^*) exceeding 10^{12} Jones at 20 kHz, which rival those of lead- or mercury-based counterparts while adhering to environmental regulations (Fig. 2(c)). The Ag_2Te CQD SWIR PDs demonstrate broad spectral sensitivity from 350 nm to 1600 nm, holding the potential up to 1940 nm with tunable absorption peaks.

Furthermore, a monolithically integrated SWIR imager using solution-processed Ag_2Te CQDs on a silicon ROIC has been demonstrated (Fig. 2(d)), achieving imaging capabilities in the 350–1600 nm range. The imager successfully visualized objects opaque in visible light, such as silicon wafers and liquid-filled bottles, under SWIR illumination (Fig. 2(e) and (f)).

Motivated by the highly demanding performance at the low-frequency regime (≈ 1 Hz) for practical applications and integration with read-out electronics, advanced surface engineering and doping control were conducted on Ag_2Te QDs to improve surface passivation and device band alignment. These improvement methods were instrumental in reducing trap states and

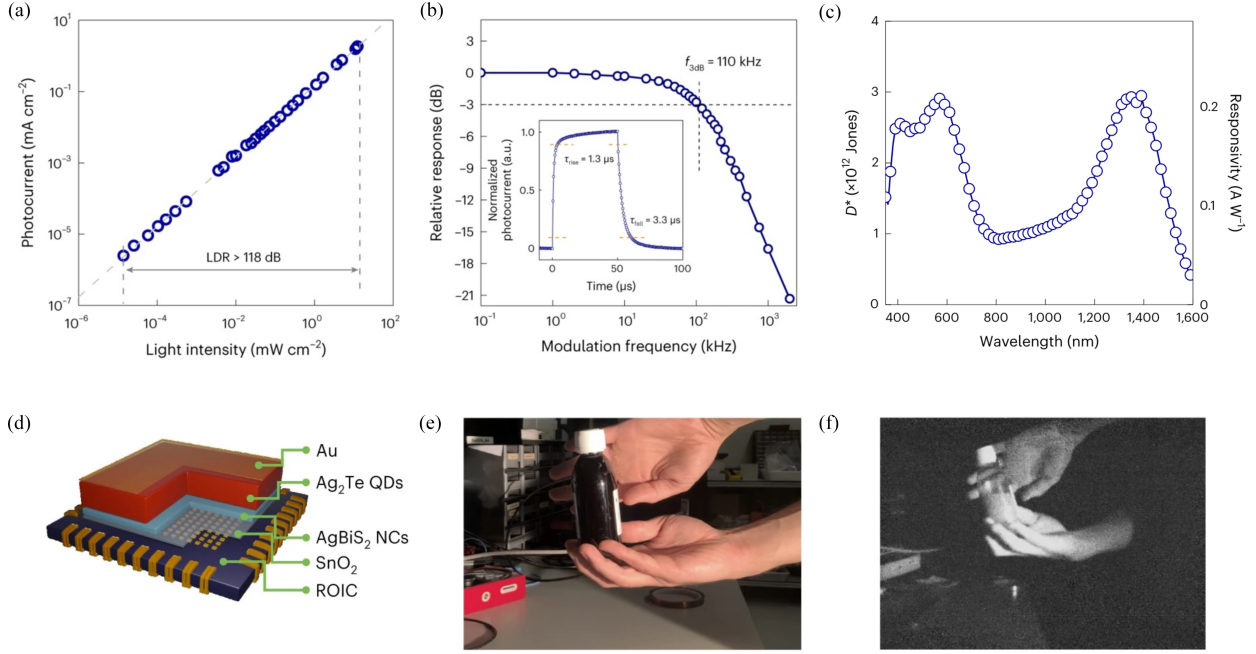


Fig. 2. (a) LDR of Ag_2Te QD photodiode under 1310 nm pulse light illumination with power densities from $\sim 10 \text{ nW cm}^{-2}$ to $\sim 10 \text{ mW cm}^{-2}$. (b) Response bandwidth of Ag_2Te QD photodiode. (c) Specific detectivity spectrum at 20 kHz. (d) Schematic of ROIC-integrated Ag_2Te QD SWIR imager. Photographs of a dark bottle with a liquid using the smartphone's visible camera (e) and the Ag_2Te QD SWIR camera (f). Figures reproduced with permission from Springer Nature ([16]).

enabling uniform charge transport, which directly contributed to the superior device performance. The fabricated devices exhibited a dark current density of approximately 450 nA cm^{-2} at -0.5 V (Fig. 3(a)), external quantum efficiencies exceeding 30%, and a linear dynamic range above 150 dB (Fig. 3(b)), while transient photocurrent measurements revealed a response time of around 25 ns (Fig. 3(c)). Furthermore, a proof-of-concept SWIR LiDAR demonstration was performed using a 1310 nm nanosecond diode laser, achieving decimetre-level resolution over distances exceeding 10 m (Fig. 3(d) and (e)). These achievements highlight the potential of Ag_2Te CQDs as a sustainable, high-performance alternative for SWIR applications in automotive sensing, machine vision, and consumer electronics.

B. Ag_2Te CQDs for eSWIR

Ag_2Te CQDs, with their versatile bandgap tunability, can be employed for applications in extended shortwave infrared (eSWIR) region (Fig. 4(a)) [28]. Ahn et al. have reported an eSWIR photodetector using Ag_2Te CQDs (Fig. 4(b) and (c)). They leveraged thiolate ligand-exchange with 3-mercaptopropionic acid (MPA), 2-mercaptoethanol (ME) and 12-ethanedithiol (EDT) (Fig. 4(d)), enabling a lower trap density and improved carrier mobility in CQD solids. They have achieved high-quality rectification with a low dark current density of 10^{-4} A/cm^2 at -1 V reverse bias (Fig. 4(c)), and a fast response time of 72 ns. However, as shown in Fig. 4(d) and (e), the devices showed a low EQE ($< 1\%$) and detectivity ($\sim 10^7$ Jones), hence significant efforts are needed to further improve and enhance the potential of Ag_2Te CQDs for eSWIR applications. Kim et al further developed a solution-phase ligand-exchange process for Ag_2Te CQD inks using engineered surface binding

ligand [29], and further studied the combination of the halide composition of the ink (Fig. 5(a) and (b)) and demonstrate that it significantly influences the device dark current due to improved mobility and trap density (Fig. 5(c)). By applying a mixture of chloride (TBACl) and iodide (TBAI), they have achieved a photo-response fall time of $2.7 \mu\text{s}$ (Fig. 5(d)), an EQE of 16% at -0.3 V bias (Fig. 5(e)), and a specific detectivity (D^*) of 9.0×10^{10} Jones at room temperature at $1.7 \mu\text{m}$ (Fig. 5(f)).

These results emphasize the potential of Ag_2Te QDs for extending the photodetection capabilities into the eSWIR range as less-toxic materials than heavy-metal based lead/mercury chalcogenide CQDs.

C. III-V CQDs

Apart from silver chalcogenide CQDs, III-V group semiconductor quantum dots have also shown steady rising as heavy-metal-free contenders for high performance shortwave infrared photodetectors [25], [33], [39], [40], [41].

A key development lies in the surface passivation techniques to address the covalent nature of III-V CQDs. For InAs CQDs, surface engineering has improved the device performance with 37% EQE at 950 nm and a detectivity of 1.9×10^{11} Jones [23], [40], [41], [42]. A mixed-halide passivation strategy has also been developed for large InAs CQDs, leading to a T90 lifetime of 50 h, an EQE of 75% and a response time of 10 ns, an advance for InAs photodetectors operating at 1140 nm [43]. InSb CQDs possess narrower bandgap than InAs CQDs, presenting even more promising potential in the shortwave infrared region. Halide-driven synthesis using ZnX_2 ($\text{X} = \text{F}, \text{Br}, \text{I}$) additives decelerates antimony precursor reduction [44], enabling precise size control and narrow size distributions of InSb CQDs. This

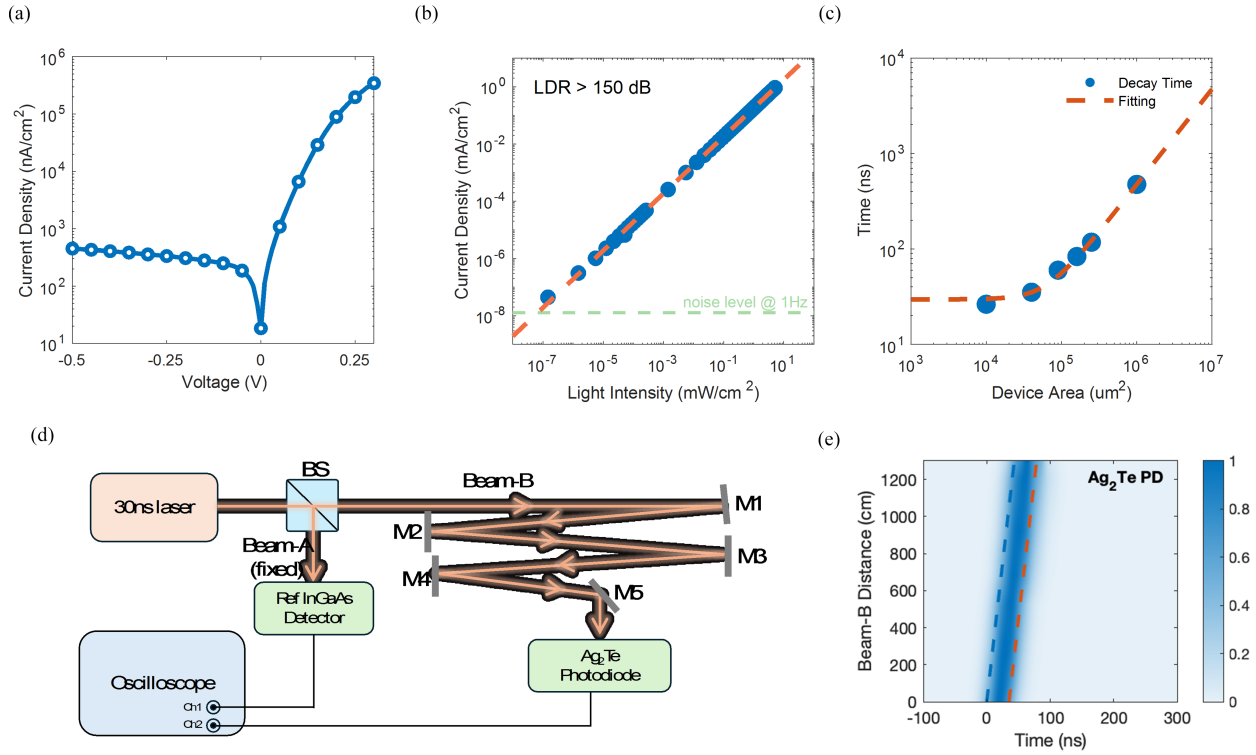


Fig. 3. (a) Dark current density–voltage curve of the Ag₂Te CQD device. (b) Linear dynamic range (LDR) of Ag₂Te QD photodiode under 1350 nm light. (c) Response speed of Ag₂Te QD photodiodes with varying device area. (d) Schematic of the homemade LiDAR set-up. (e) Contour plot of the signal transient from Ag₂Te QD photodiodes. Figures reproduced with permission from Wiley-VCH GmbH [17].

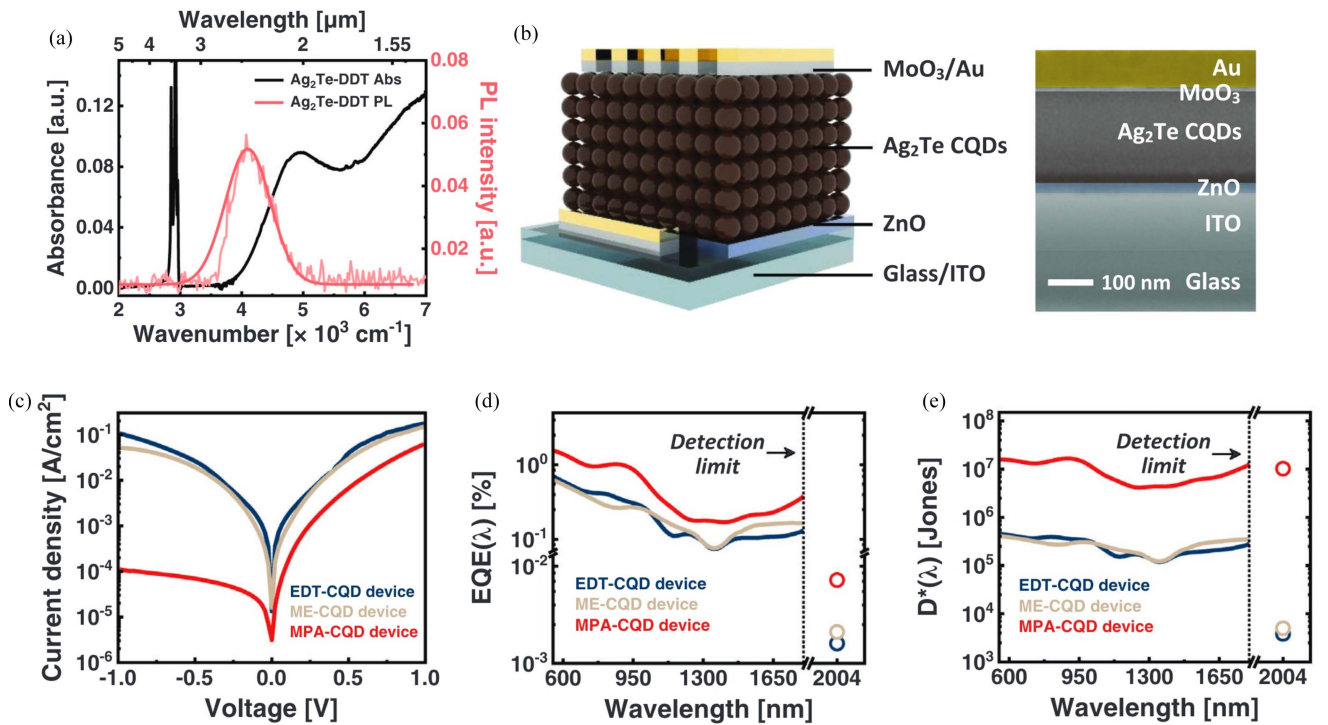


Fig. 4. (a) Absorbance and infrared PL spectra of the DDT-capped Ag₂Te CQDs. (b) Device architecture and a cross-sectional SEM image. (c) Current density–voltage (J – V) curves of EDT-, ME-, and MPA-CQD devices under dark conditions. (d) EQE spectra of EDT, ME, and MPA-CQD devices. (e) D^* spectra of EDT-, ME-, and MPA-CQD devices. Figures reproduced with permission from Wiley-VCH GmbH [28].

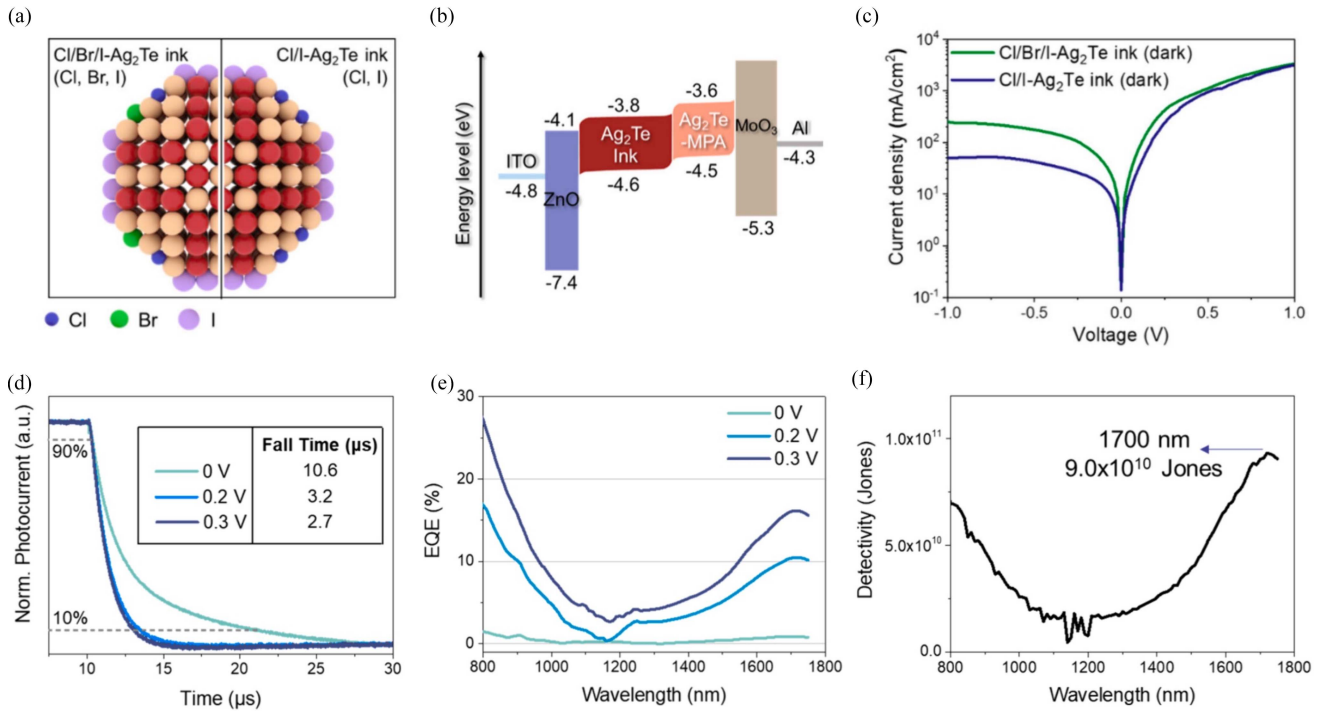


Fig. 5. (a) Schematic representation of Ag₂Te CQD inks with different combinations of the halide ligands. (b) Energy level alignment of Ag₂Te photodetector device. (c) $J-V$ curves of Ag₂Te CQD ink device under dark conditions. (d) Voltage dependent photo-response spectra of Cl/I-Ag₂Te photodetector. (e) EQE spectra of Cl/I-Ag₂Te photodetector device at bias voltages of 0, 0.2, and 0.3 V. (f) Detectivity of Cl/I-Ag₂Te photodetector at 0.3 V bias voltage. Figures reproduced with permission from American Chemical Society ([29]).

synthetic advance highlights the role of halides in balancing reaction kinetics and surface passivation [33], [44].

In addition to surface passivation, core-shell structures could potentially provide ‘quasi-epitaxial’ interface with reduction of exciton-phonon coupling. InP shell has been shown significantly enhancing PL intensity of InSb CQDs [25]. Photodetectors based on core-shell InSb/InP core-shell CQDs has demonstrated a low dark current at reverse bias as 0.3 mA/cm² and a maximum EQE of 25% at 1240 nm. The devices also showed a fast photo-response time and a -3 dB bandwidth up to 6MHz and a specific detectivity of up to 4.4×10^{11} Jones, which remarked first solution-processed photodetector based on InSb, with figures of merit that are comparable with other CQD materials, highlighting the tremendous potential of InSb CQDs as a heavy-metal-free active material for SWIR photodetectors.

Recently, imagers based on InAs QDs as alternative for 1st generation Pb-based stacks have been reported by Song et al and Enoki et al [26], [27]. Novel synthesis method yields 9 nm InAs QDs optimized for 1400 nm and solution-phase ligand exchange results in uniform single-step coating. Demonstrated EQE over 17.4% and >300 hours air-stability promise compatibility with fab manufacturing. These results stand as starting point towards the 2nd generation quantum dot SWIR imagers.

III. DISCUSSIONS AND PERSPECTIVES

Heavy-metal-free CQDs bridge the gap between high-performance SWIR photodetection and environmental sustainability. Table I captures the current state-of-the-art in heavy-metal-free CQD SWIR Photodiodes. Their compatibility with silicon substrates overcomes the need for costly heterogeneous

interconnection processes, enabling low-cost, scalable production of infrared sensors, unlocking applications in consumer electronics, autonomous vehicles, and wearable health monitors. However, achieving industrial-scale production requires addressing material synthesis scalability, probably through automated or continuous-flow reactors rather than small-batch lab-scale synthesis. Furthermore, considerations about the compatibility of CQD materials with existing CMOS infrastructure should be taken into account for future industrial adoption. Ag-based CQDs might face in-operando stability challenges due to the nature of Ag⁺ ions under applied bias conditions and may require dedicated surface stabilization strategies to mitigate such effects. Also the use of chalcogens needs to be evaluated on possible contamination issues of Si CMOS foundries and appropriate strategies would need to be adopted. Similarly, albeit arsenic-containing CQDs (e.g., InAs), are expected to be more stable -in view of their covalent nature- compared to their heavy metal ionic counterparts (e.g., Pb-chalcogenides), concerns about safety and sustainability on their manufacturing and recycling processes, by generating airborne nanoparticles or liquid waste requiring stringent disposal protocols, need to be addressed as the technology matures.

Current challenges include limited EQE in SWIR regimes, environmental instability of CQDs, and higher dark currents compared to InGaAs. Future research should prioritize ligand engineering to reduce trap states and explore hybrid architectures to enhance carrier extraction and responsivity. Beyond initial performance metrics, long-term reliability under operational conditions remains an open question for CQD based photodetectors. Developing robust encapsulation might be paramount.

TABLE I
SUMMARY OF HEAVY-METAL-FREE CQD SWIR PHOTODIODE PERFORMANCE SINCE YEAR 2024

CQD Materials	J_{dark} @-0.5V $\mu\text{A}/\text{cm}^2$	J_{dark} @-1V $\mu\text{A}/\text{cm}^2$	Peak EQE @-1V %	Peak EQE @max bias reported %	D^* Jones	Response Speed μs	Ref
Ag_2Te	0.45	-	30% @ 1450nm	30% @ 1450nm	10^{11} @ 1Hz	0.025	[17]
Ag_2Te	6	~20	-	30% @ 1400nm	10^{10} @ 1Hz 3×10^{12} @ 20kHz	3.3	[16]
Ag_2Te	~80	110	-	0.2% @ 1550nm	10^7 @ 10kHz	0.072	[28]
Ag_2Te	>30000	~50000	-	16% @ 1700nm	9×10^{10} @ 10kHz	2.7	[29]
InAs	~0.1	~0.1	33.5% @ 1020nm	43% @ 1020nm	1.6×10^{10} @ 300Hz	9	[30]
InAs	~3	10	15% @ 1450nm	15% @ 1450nm	1.2×10^{10} @ 10Hz	1	[31]
InAs	~0.03	0.01	40% @ 940nm	40% @ 940nm	-	< 30	[26]
	~10	~50	~12% @ 1450nm	15% @ 1450nm	-	< 30	[26]
InAs	~100	~200	-	17.4% @ 1390nm	9.3×10^9 @ shot noise	-	[27]
InSb	~8	9.6	25% @ 1400nm	25% @ 1400nm	1.4×10^{11} @ 100kHz	5.6	[32]
InSb	~80	~200	~17% @ 1240nm	25% @ 1240nm	4.4×10^{11} @ 10kHz	0.07	[25]
InSb	~3	14.4	33% @ 1380nm	33% @ 1380nm	10^{12} @ 2kHz	1.4	[33]

Besides, accelerated aging tests under high humidity, temperature, and SWIR illumination are needed to establish industry-standard reliability benchmarks. In doing so, most likely new ligand chemistries are required to facilitate very low trap-state density, thus low dark current and long minority carrier lifetime, as well as high carrier mobility to warrant high quantum efficiency. Additionally, such ligand chemistries should be robust enough to lend devices temperature and environmental resilience.

Advancements in synthetic control, interfacial engineering, and device scalability will drive heavy-metal-free CQDs toward commercial viability. Targets include achieving detectivity $>10^{13}$ Jones, nanosecond response times, and multi-spectral imaging capabilities. Collaborative efforts between academia and industry are essential to translate laboratory breakthroughs into market-ready technologies.

IV. CONCLUSION

The rapid evolution of heavy-metal-free CQDs marks a paradigm shift in infrared photodetection. Silver chalcogenides and III-V semiconductors have demonstrated exceptional performance, with Ag_2Te CQDs achieving room-temperature detectivity surpassing 10^{12} Jones and III-V devices reaching EQE values exceeding 75%. These materials not only comply with stringent environmental regulations but also enable cost-effective, large-area sensor production through solution processing. Despite lingering challenges in quantum efficiency, dark-current and long-term stability, recent advances in surface passivation, ligand engineering, and monolithic integration underscore their transformative potential. By addressing current limitations, heavy-metal-free CQDs are poised to redefine infrared technologies, fostering advancements in consumer electronics, industrial automation, and biomedical diagnostics. This progress aligns with global sustainability goals, paving the

way for a future where high-performance optoelectronics could potentially coexist with environmental responsibility.

V. CONFLICT OF INTEREST

G. K. serves as cofounder, shareholder and member of the board of directors of Qurv Technologies S.L.

REFERENCES

- [1] H. Yang, Z. Ma, and Q. Wang, "Shortwave-infrared silver chalcogenide quantum dots for optoelectronic devices," *ACS Nano*, vol. 18, pp. 30123–30131, Oct. 2024, doi: [10.1021/acsnano.4c11787](https://doi.org/10.1021/acsnano.4c11787).
- [2] J. Du et al., "Review of short-wavelength infrared flip-chip bump bonding process technology," *Sensors*, vol. 25, no. 1, Jan. 2025, Art. no. 263, doi: [10.3390/s25010263](https://doi.org/10.3390/s25010263).
- [3] Y. Xie et al., "Bright short-wavelength infrared organic light-emitting devices," *Nature Photon.*, vol. 16, no. 11, pp. 752–761, Nov. 2022, doi: [10.1038/s41566-022-01069-w](https://doi.org/10.1038/s41566-022-01069-w).
- [4] G. Konstantatos et al., "Ultrasensitive solution-cast quantum dot photodetectors," *Nature*, vol. 442, no. 7099, pp. 180–183, Jul. 2006, doi: [10.1038/nature04855](https://doi.org/10.1038/nature04855).
- [5] G. Konstantatos, J. Clifford, L. Levina, and E. H. Sargent, "Sensitive solution-processed visible-wavelength photodetectors," *Nature Photon.*, vol. 1, no. 9, pp. 531–534, Sep. 2007, doi: [10.1038/nphoton.2007.147](https://doi.org/10.1038/nphoton.2007.147).
- [6] S. A. McDonald et al., "Solution-processed PbS quantum dot infrared photodetectors and photovoltaics," *Nature Mater.*, vol. 4, no. 2, pp. 138–142, Feb. 2005, doi: [10.1038/nmat1299](https://doi.org/10.1038/nmat1299).
- [7] F. P. García De Arquer, A. Armin, P. Meredith, and E. H. Sargent, "Solution-processed semiconductors for next-generation photodetectors," *Nature Rev. Mater.*, vol. 2, no. 3, Jan. 2017, Art. no. 16100, doi: [10.1038/natrevmats.2016.100](https://doi.org/10.1038/natrevmats.2016.100).
- [8] J. Liu et al., "A near-infrared colloidal quantum dot imager with monolithically integrated readout circuitry," *Nature Electron.*, vol. 5, no. 7, pp. 443–451, Jul. 2022, doi: [10.1038/s41928-022-00779-x](https://doi.org/10.1038/s41928-022-00779-x).
- [9] X. Tang, M. M. Ackerman, M. Chen, and P. Guyot-Sionnest, "Dual-band infrared imaging using stacked colloidal quantum dot photodiodes," *Nature Photon.*, vol. 13, no. 4, pp. 277–282, Apr. 2019, doi: [10.1038/s41566-019-0362-1](https://doi.org/10.1038/s41566-019-0362-1).
- [10] R. Chang, Q. Xu, Q. Yin, X. Yang, Z. Wu, and H. Shen, "High-performance photodiodes based on In-situ etched PbSe colloidal quantum dots with responses extended to 2500 nm," *Nano Lett.*, vol. 24, pp. 15845–15851, Nov. 2024, doi: [10.1021/acs.nanolett.4c04787](https://doi.org/10.1021/acs.nanolett.4c04787).

- [11] D. Chen et al., "Passivating {100} facets of PbS colloidal quantum dots via perovskite bridges for sensitive and stable infrared photodiodes," *Adv. Funct. Mater.*, vol. 33, no. 1, 2023, Art. no. 2210158, doi: [10.1002/adfm.202210158](https://doi.org/10.1002/adfm.202210158).
- [12] J. S. Steckel et al., "1.62 μ m global shutter quantum dot image sensor optimized for near and shortwave infrared," in *Proc. 2021 IEEE Int. Electron Devices Meeting*, Dec. 2021, pp. 23.4.1–23.4.4, doi: [10.1109/IEDM19574.2021.9720560](https://doi.org/10.1109/IEDM19574.2021.9720560).
- [13] X. Zhao, L. J. Lim, S. S. Ang, and Z. -K. Tan, "Efficient short-wave infrared light-emitting diodes based on heavy-metal-free quantum dots," *Adv. Mater.*, vol. 34, no. 45, 2022, Art. no. 2206409, doi: [10.1002/adma.202206409](https://doi.org/10.1002/adma.202206409).
- [14] X. Zhang, G. Mu, Y. Zhang, Y. Jiang, and Y. Yan, "Heavy metal-free colloidal quantum dots: Preparation and application in infrared photodetectors," *J. Mater. Chem. C*, vol. 12, pp. 15811–15832, 2024, doi: [10.1039/D4TC03312D](https://doi.org/10.1039/D4TC03312D).
- [15] Z. Wang, F. Liu, Y. Gu, Y. Hu, and W. Wu, "Solution-processed self-powered near-infrared photodetectors of toxic heavy metal-free AgAuSe colloidal quantum dots," *J. Mater. Chem. C*, vol. 10, no. 3, pp. 1097–1104, Jan. 2022, doi: [10.1039/D1TC03837K](https://doi.org/10.1039/D1TC03837K).
- [16] Y. Wang et al., "Silver telluride colloidal quantum dot infrared photodetectors and image sensors," *Nature Photon.*, vol. 18, no. 3, pp. 236–242, Mar. 2024, doi: [10.1038/s41566-023-01345-3](https://doi.org/10.1038/s41566-023-01345-3).
- [17] Y. Wang et al., "Shortwave infrared light detection and ranging using silver telluride quantum dots," *Adv. Mater.*, vol. 35, 2025, Art. no. 2500977, doi: [10.1002/adma.202500977](https://doi.org/10.1002/adma.202500977).
- [18] J. Leemans et al., "Acid–base mediated ligand exchange on near-infrared absorbing, indium-based III–V colloidal quantum dots," *J. Amer. Chem. Soc.*, vol. 143, no. 11, pp. 4290–4301, Mar. 2021, doi: [10.1021/jacs.0c12871](https://doi.org/10.1021/jacs.0c12871).
- [19] I. Burgués-Ceballos, Y. Wang, and G. Konstantatos, "Mixed AgBiS₂ nanocrystals for photovoltaics and photodetectors," *Nanoscale*, vol. 14, no. 13, pp. 4987–4993, 2022, doi: [10.1039/D2NR00589A](https://doi.org/10.1039/D2NR00589A).
- [20] Y. Wang, S. R. Kavanagh, I. Burgués-Ceballos, A. Walsh, D. O. Scanlon, and G. Konstantatos, "Cation disorder engineering yields AgBiS₂ nanocrystals with enhanced optical absorption for efficient ultrathin solar cells," *Nature Photon.*, vol. 16, no. 3, pp. 235–241, Mar. 2022, doi: [10.1038/s41566-021-00950-4](https://doi.org/10.1038/s41566-021-00950-4).
- [21] Y. -T. Huang et al., "Fast near-infrared photodetectors based on non-toxic and solution-processable AgBiS₂," *Small*, vol. 20, no. 18, 2024, Art. no. 2310199, doi: [10.1002/smll.202310199](https://doi.org/10.1002/smll.202310199).
- [22] Y. Miao, Z. Wang, Z. Wei, and G. Shen, "Patterned growth of AgBiS₂ nanostructures on arbitrary substrates for broadband and eco-friendly optoelectronic sensing," *Nanoscale*, vol. 16, no. 15, pp. 7409–7418, 2024, doi: [10.1039/D4NR00499J](https://doi.org/10.1039/D4NR00499J).
- [23] P. Xia et al., "Sequential co-passivation in InAs colloidal quantum dot solids enables efficient near-infrared photodetectors," *Adv. Mater.*, vol. 35, no. 28, 2023, Art. no. 2301842, doi: [10.1002/adma.202301842](https://doi.org/10.1002/adma.202301842).
- [24] B. Sun et al., "Fast near-infrared photodetection using III–V colloidal quantum dots," *Adv. Mater.*, vol. 34, no. 33, 2022, Art. no. 2203039, doi: [10.1002/adma.202203039](https://doi.org/10.1002/adma.202203039).
- [25] L. Peng, Y. Wang, Y. Ren, Z. Wang, P. Cao, and G. Konstantatos, "InSb/InP core–shell colloidal quantum dots for sensitive and fast short-wave infrared photodetectors," *ACS Nano*, vol. 18, no. 6, pp. 5113–5121, Feb. 2024, doi: [10.1021/acs.nano.3c12007](https://doi.org/10.1021/acs.nano.3c12007).
- [26] O. Enoki et al., "Pb-free colloidal InAs quantum dot image sensor for infrared," in *Proc. 2024 IEEE Int. Electron Devices Meeting*, Dec. 2024, pp. 1–4, doi: [10.1109/IEDM50854.2024.10873373](https://doi.org/10.1109/IEDM50854.2024.10873373).
- [27] W. Song et al., "Lead-free quantum dot photodiodes for next generation short wave infrared optical sensors," in *Proc. 2024 IEEE Int. Electron Devices Meeting*, Dec. 2024, pp. 1–4, doi: [10.1109/IEDM50854.2024.10873395](https://doi.org/10.1109/IEDM50854.2024.10873395).
- [28] Y. Ahn et al., "Silver telluride colloidal quantum dot solid for fast extended shortwave infrared photodetector," *Adv. Sci.*, vol. 11, 2024, Art. no. 2407453, doi: [10.1002/adv.202407453](https://doi.org/10.1002/adv.202407453).
- [29] G. Kim et al., "Extended short-wavelength infrared ink by surface-tuned silver telluride colloidal quantum dots and their infrared photodetection," *ACS Mater. Lett.*, vol. 25, pp. 4988–4996, Oct. 2024, doi: [10.1021/acsmaterialslett.4c01585](https://doi.org/10.1021/acsmaterialslett.4c01585).
- [30] B. K. Jung et al., "High-affinity ligand-enhanced passivation of group III–V colloidal quantum dots for sensitive near-infrared photodetection," *ACS Energy Lett.*, vol. 9, no. 2, pp. 504–512, Feb. 2024, doi: [10.1021/acsenenergylett.3c02515](https://doi.org/10.1021/acsenenergylett.3c02515).
- [31] T. Sheikh et al., "Surface-reconstructed InAs colloidal nanorod quantum dots for efficient deep-shortwave infrared emission and photodetection," *J. Amer. Chem. Soc.*, vol. 146, no. 42, pp. 29094–29103, Oct. 2024, doi: [10.1021/jacs.4c10755](https://doi.org/10.1021/jacs.4c10755).
- [32] Y. Zhang et al., "Dicarboxylic acid-assisted surface oxide removal and passivation of indium antimonide colloidal quantum dots for short-wave infrared photodetectors," *Angewandte Chemie*, vol. 136, no. 8, 2024, Art. no. e202316733, doi: [10.1002/ange.202316733](https://doi.org/10.1002/ange.202316733).
- [33] M. Imran et al., "Control over metal-halide reactivity enables uniform growth of InSb colloidal quantum dots for enhanced SWIR light detection," *Adv. Mater.*, vol. 37, 2025, Art. no. 2420273, doi: [10.1002/adma.202420273](https://doi.org/10.1002/adma.202420273).
- [34] Z. -Y. Liu et al., "Breaking through the size control dilemma of silver chalcogenide quantum dots via trialkylphosphine-induced ripening: Leading to Ag₂Te emitting from 950 to 2100 nm," *J. Amer. Chem. Soc.*, vol. 143, no. 32, pp. 12867–12877, Aug. 2021, doi: [10.1021/jacs.1c06661](https://doi.org/10.1021/jacs.1c06661).
- [35] M. -Y. Zhang et al., "Regulation of silver precursor reactivity via tertiary phosphine to synthesize near-infrared Ag₂Te with photoluminescence quantum yield of up to 14.7%," *Chem. Mater.*, vol. 33, no. 24, pp. 9524–9533, Dec. 2021, doi: [10.1021/acs.chemmater.1c02610](https://doi.org/10.1021/acs.chemmater.1c02610).
- [36] Z. Li et al., "Interface nucleophilic substitution reaction-driven precise growth of Ag₂Te quantum dots," *Chem. Mater.*, vol. 36, no. 19, pp. 9341–9355, Oct. 2024, doi: [10.1021/acs.chemmater.4c00026](https://doi.org/10.1021/acs.chemmater.4c00026).
- [37] J. Ouyang et al., "Ag₂Te colloidal quantum dots for near-infrared-II photodetectors," *ACS Appl. Nano Mater.*, vol. 4, no. 12, pp. 13587–13601, Dec. 2021, doi: [10.1021/acsanm.1c03030](https://doi.org/10.1021/acsanm.1c03030).
- [38] G. Kim, D. Choi, S. Y. Eom, H. Song, and K. S. Jeong, "Extended short-wavelength infrared photoluminescence and photocurrent of non-stoichiometric silver telluride colloidal nanocrystals," *Nano Lett.*, vol. 21, no. 19, pp. 8073–8079, Oct. 2021, doi: [10.1021/acs.nanolett.1c02407](https://doi.org/10.1021/acs.nanolett.1c02407).
- [39] W. J. Mir et al., "One-pot colloidal synthesis enables highly tunable InSb short-wave infrared quantum dots exhibiting carrier multiplication," *Small*, vol. 20, no. 19, 2024, Art. no. 2306535, doi: [10.1002/smll.202306535](https://doi.org/10.1002/smll.202306535).
- [40] H. W. Ban et al., "Resurfacing of InAs colloidal quantum dots equalizes photodetector performance across synthetic routes," *J. Amer. Chem. Soc.*, vol. 146, no. 36, pp. 24935–24944, Sep. 2024, doi: [10.1021/jacs.4c06202](https://doi.org/10.1021/jacs.4c06202).
- [41] M. S. Skorotetsky et al., "Si-H hydrosilane reducing agents for size- and shape-controlled InAs colloidal quantum dots," *Adv. Mater.*, vol. 37, 2025, Art. no. 2412105, doi: [10.1002/adma.202412105](https://doi.org/10.1002/adma.202412105).
- [42] D. Shin, H. Jeong, J. Kim, E. Jang, Y. Park, and S. Jeong, "High performance infrared InAs colloidal quantum dot photodetector with 79% EQE enabled by an extended absorber layer," *Adv. Opt. Mater.*, vol. 13, no. 1, 2025, Art. no. 2401931, doi: [10.1002/adom.202401931](https://doi.org/10.1002/adom.202401931).
- [43] P. Xia et al., "Improved facet and edge passivation in near-infrared III–V colloidal quantum dot photodetectors," *Adv. Mater.*, vol. 32, 2025, Art. no. 2419020, doi: [10.1002/adma.202419020](https://doi.org/10.1002/adma.202419020).
- [44] D. Muhammad et al., "Halide-driven synthetic control of InSb colloidal quantum dots enables short-wave infrared photodetectors," *Adv. Mater.*, vol. 35, no. 46, 2023, Art. no. 2306147, doi: [10.1002/adma.202306147](https://doi.org/10.1002/adma.202306147).